Carpathian Journal of Earth and Environmental Sciences, February 2026, Vol. 21, No. 1, p. 189 – 204; DOI:10.26471/cjees/2026/021/362

THE PRECIPITATION PUZZLE: A TEST OF THE NASA POWER MODEL AGAINST TUNISIAN GROUND OBSERVATIONAL DATA

Safouane MOUELHI[1], Sabri KANZARI[1], Samir GHANNEM[2], Sana BEN MARIEM[1], Kaouther BENYAHIA[1], Essaid BILAL[3*] & Mohamed Ali BEN ABDALLAH[1]

[1]National Institute of Research of Rural Engineering, Waters and Forests of Tunis, University of Carthage, Ariana, Tunisia

[2]Laboratory of Environment Biomonitoring, Faculty of Sciences of Bizerte, Jarzouna 7021, University of Carthage, Tunisia.

[3]Ecole Nationale Supérieure des Mines de Saint-Étienne, CNRS-UMR6425, Saint-Étienne, France.

**Corresponding author: ebilal@mines-stetienne.fr*

Abstract: The NASA Prediction of Worldwide Energy Resources (POWER) system delivers globally consistent, satellite-based climate and solar data that support applications in renewable energy, agriculture, and hydrology. Its open access and robust processing chain have made it a widely used source of long-term environmental information for both scientists and decision-makers. This study evaluates NASA POWER precipitation estimates against observations from 23 meteorological stations across Tunisia for the period 1981–2023. The network covers sites located in humid, semi-arid, and Saharan climate regimes. The analysis included regression performed by station and by month. Descriptive statistics were also used to describe the main features of rainfall variability. This framework allowed the assessment of both average performance and the ability of the product to reproduce interannual and spatial variability. Results show that NASA POWER reproduces the large-scale spatial pattern of mean annual rainfall well, but systematically underestimates orographic extremes and markedly dampens variability, especially in summer. The relationship between NASA POWER and observed precipitation is strongest in autumn and spring ($R^2 > 0.75$), when rainfall is primarily driven by large-scale synoptic systems. In contrast, performance degrades sharply in August ($R^2 < 0.30$ at central and southern stations), reflecting the product's limited capacity to capture localized convective events. The coefficient of variation is consistently underestimated throughout the country, indicating a structural mismatch between the product's coarse spatial resolution (about 50 km) and the fine-scale characteristics of Mediterranean rainfall. These shortcomings substantially constrain the direct use of NASA POWER for hydrological and agricultural applications in water-stressed regions without local bias correction.

Keywords: precipitation, NASA POWER dataset, correlation, irregularity, Tunisia

1. INTRODUCTION

Global climate datasets have evolved steadily over the course of several decades. Starting with World Meteorological Organization (WMO) standards in the mid-20th century (OMM, 1951; Peterson et al., 1998), they have continued to develop. Gridded products such as the Climatic Research Unit (CRU) datasets followed suit (Harris et al., 2014). Modern reanalyses, including ERA5 (Hersbach et al., 2023), built on this foundation. Nowadays, open platforms such as National Oceanic and Atmospheric Administration (NOAA) Climate Data and NASA Earth data provide free access to data (Rienecker et al., 2011; Menne et al., 2012). This has been made possible by increased computing power, improved connectivity and open data policies (Edwards et al., 2011; World Meteorological Organization (WMO), 2022). These tools now support research in many different fields.

The NASA POWER dataset has emerged as a key player. It provides global coverage, offering easy online access to reliable long-term records. Originally designed for energy needs, such as solar resource

planning (Quansah et al., 2024; Zhang et al., 2009), it now supports climate services (Jing et al., 2019), as well as agriculture, hydrology, and climatology.

In the field of agriculture and irrigation, variables such as temperature, solar radiation, and reference evapotranspiration (ETo) have been evaluated and applied for crop modelling and water management in countries including Brazil, Portugal, and Egypt (Monteiro et al., 2018; Aboelkhair et al., 2019; Rodrigues & Braga, 2021b). In hydrology, the dataset is used for streamflow modelling, precipitation studies, and drought detection, particularly in regions where ground observations are scarce (Jiménez-Jiménez et al., 2021; Kheyruri & Sharafati, 2022; Kadhim Tayyeh & Mohammed, 2023; Asilevi et al., 2024). In climatology, it supports analyses of temperature trends and climate variability in arid, semi-arid, aridity and drought, and the interaction between climate and terrain characteristics (Sarfaraz, 2017; Célestin et al., 2019; Abubakar & Idi, 2024; Matallah et al., 2025; Bensefia et al., 2026).

In Tunisia, the utilization of NASA POWER data has expanded rapidly, providing substantial support to numerous research disciplines. For instance, Ben Othman et al. (2020) utilized POWER data to estimate photovoltaic potential under climate change scenarios by employing deep learning methods in the El Akarit region. Mouelhi et al. 2025 combined POWER data with other information to build a parametric classification of Tunisian dams and improve water scarcity management. Serbaji et al. 2023) applied a GIS-RUSLE framework with POWER-based climate variables to model soil erosion risk. Farhani et al. 2022 utilized POWER reanalysis as a consistent climate input to analyze multispectral drought indices in central Tunisia. Gharnouki et al. (2024) also assessed the performance of satellite and reanalysis rainfall products in a Tunisian catchment with a semi-arid climate.

Despite its widespread use, several limitations of the NASA POWER dataset have been reported. In Mediterranean conditions, such as the Alentejo region in southern Portugal, there is a strong correlation between temperature and solar radiation estimates and ground observations. However, wind speed remains poorly represented, even after bias correction. A systematic error has also been identified in evapotranspiration estimates. This bias is linked to errors in humidity and wind data and makes local calibration necessary before using the product with confidence (Rodrigues & Braga, 2021b, 2021a) In tropical climates, NASA POWER dataset does not correctly represent precipitation and temperature extremes, so additional corrections are required (Tan et al., 2023). The model also has a tendency to underestimate heavy rainfall in West Africa, which has a detrimental effect on its usefulness for drought monitoring in that region (Dawa et al., 2024).

In Tunisia, despite the growing use of NASA POWER, the reliability of its precipitation remains unvalidated on a national scale. This gap persists as rainfall variability dictates agricultural yields and water security (Latiri et al., 2010). Accurate representation is hindered by localised convective events and orographic influences, which regional and global models often fail to capture, particularly in Northern and semi-arid basins (Bargaoui et al., 2014; Gharnouki et al., 2024). In water-scarce regions, such discrepancies can bias hydrological modelling and decision-making processes (MAWRF, 2022). Consequently, this study evaluates the product (1981–2023) across 23 stations. The specific objectives are to: (i) assess performance against interannual monthly distributions, (ii) evaluate the reproduction of spatial rainfall patterns, and (iii) develop month-specific regression adjustments to correct local variability.

2. MATERIALS AND METHODS

Figure 1 provides an overview of the research process. The work is organized into three main steps. First, we collect and describe the observed rainfall data from the Tunisian General Directorate of Water Resources (DGRE) station network. Second, we extract matching data from the NASA POWER model for the same sites and time period. Thirdly, we compare the two datasets using regression analysis to evaluate the model's performance. Finally, we discuss the main implications and directions for future studies.

2.1. Database construction

The NASA POWER project (*NASA POWER | Prediction Of Worldwide Energy Resources*, 2025) provides several agroclimatic variables at different spatial and temporal scales. Temperature estimates from this dataset are generally reliable, with the coefficient of determination often above 0.9. Rainfall estimates, however, show lower agreement in many initial evaluations. NASA POWER precipitation data are derived entirely from the GPM IMERG (Global Precipitation Measurement – Integrated Multi-satellite Retrievals for GPM) “Final” product. This dataset includes gauge-based corrections to improve accuracy, but satellite rainfall measurements are still indirect and can be influenced by factors such as terrain, rainfall intensity, and climate conditions. These uncertainties are then carried into the NASA

POWER dataset. In most cases, the performance of such global products is assessed at the worldwide scale using large international networks of ground stations. As a result, the reported biases reflect global averages and may not properly represent the specific errors and uncertainties that exist in a given region, such as Tunisia.

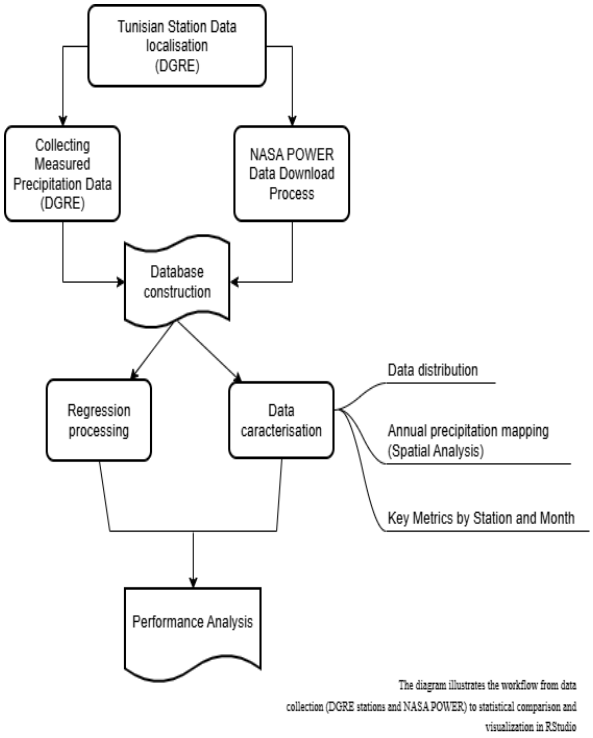

Figure 1. Diagram of the methodological framework.

Building on the rationale presented in the introduction, where precipitation was highlighted as the key variable due to its crucial role in water management and its high impact in arid and semi-arid regions, it is worth noting here the sensitivity of rainfall-runoff models to precipitation. Accurate rainfall data are essential because runoff models are highly sensitive to precipitation, much more than to other meteorological inputs. In fact, runoff responses can amplify rainfall variations by two to five times (Chiew et al., 2005; Ghane et al., 2017; Liu et al., 2024). This sensitivity is even greater because rainfall varies so much across space and time, especially during intense convective events. For this reason, precipitation is widely considered the most critical and uncertain input in hydrological models, more so than temperature, evapotranspiration, or other factors (Bell & Moore, 2000; Hohmann et al., 2020). Due to this combination of high sensitivity and substantial uncertainty, precipitation was chosen as the variable for this evaluation. The process of building a robust reference database for this study is described below.

This assessment used the observation network of the DGRE, which operates under the Tunisian Ministry of Agriculture, Water Resources and Fisheries (MARHP). The network includes several dozen hydro-pluviometric stations. The final selection of stations was based on three main criteria: (1) Data record length: only series extending back to at least January 1981 were considered, to match the NASA POWER archive; (2) Data completeness: stations with missing values between 1981 and 2023 were excluded. This ensures that the evaluation relies on observed data only, eliminating the need for statistical imputation and avoiding bias from synthetic values; and (3) Spatial coverage: the chosen stations provide a representative distribution across Tunisia's varied climatic zones. The spatial distribution of the final selected station network is presented in Figure 2.

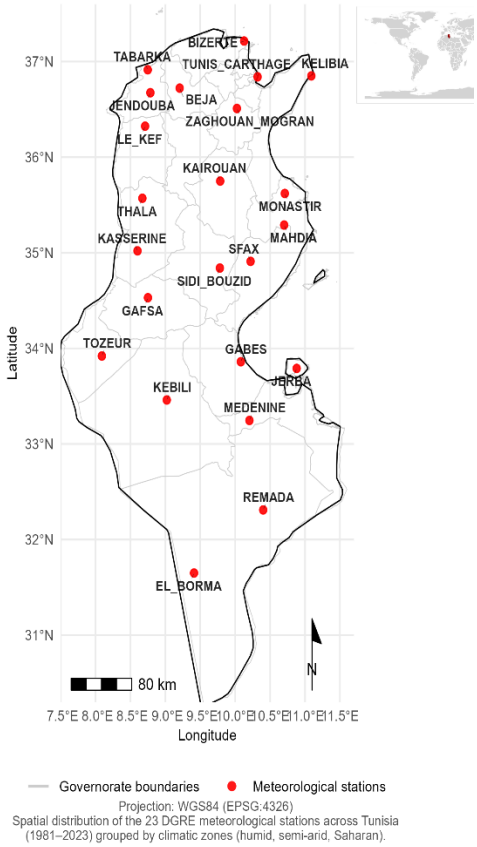

Figure 2. Spatial distribution of the selected monitoring stations.

The corresponding monthly precipitation data for the selected stations were downloaded from the NASA POWER platform using their geographic coordinates. This data was collected for the period from 1 January 1981 to 31 December 2023. This resulted in a consolidated database of monthly precipitation records for the 23 selected stations, comprising ground-based measurements and NASA POWER modelled estimates. In cases where there

were gaps in the observed records, data infilling was performed using conventional methods: regression with the nearest correlated station or insertion of the long-term average for the specific missing month.

2.2. Methodology for performance evaluation of NASA POWER precipitation data

Spatial interpolation of annual mean precipitation (both observed and NASA POWER–derived) was performed using ordinary kriging, with an exponential variogram model fitted in accordance with standard geostatistical principles and equations (Bivand et al., 2013).

To quantitatively compare the observed ground-based data with the NASA POWER-modelled estimates, this study employs regression analysis, the same approach used by NASA POWER for validation. The performance of the precipitation estimates was evaluated using two statistical metrics: the coefficient of determination (R^2) and the root mean square error (RMSE) (*NASA POWER | Prediction Of Worldwide Energy Resources*, 2025).

Regression analysis was performed using an automated iterative process to test three models for each station: linear, quadratic, and exponential. Model selection followed the principle of parsimony (Burnham & Anderson, 2002): the linear model was retained unless a more complex model (quadratic or exponential) provided a substantial improvement in the coefficient of determination. Specifically, a threshold of $\Delta R^2 < 0.05$ was applied as a penalty for model complexity; the more complex models were only selected if they increased the explained variance by at least 5% over the linear model, thereby reducing the risk of overfitting. At the station level, regressions were forced through the origin (zero intercept) to ensure physical consistency. This prevents 'phantom' rainfall and ensures that zero estimates match zero observations (Teutschbein & Seibert, 2012). For the global national regression, both models (with and without intercept) were maintained to capture the overall regional trend.

Several regression models were applied: linear, exponential, quadratic, and LOESS. To evaluate their performance, we used the coefficient of determination (R^2) and the root mean square error (RMSE), along with basic descriptive statistics such as the mean, standard deviation, and coefficient of variation. All calculations followed the standard procedures described by (Wilks, 2019).

All steps, from collecting data to producing graphs, maps, and tables, were automated with custom scripts, as depicted in Figure 1, ensuring that the methodology is fully reproducible. Furthermore, if updates are made to the NASA POWER dataset (which occurs quarterly), the entire analytical process can be seamlessly re-executed to incorporate the latest data and refresh all results. This ensures the long-term relevance and updatability of this assessment. The methodology was built within an open-source framework to support the FAIR principles of data management (findable, accessible, interoperable, and reusable; Wilkinson et al., 2016). Data processing and analyses were performed entirely in the RStudio environment (RStudio Team, 2024).

The processes of downloading data and producing graphics, tables, and maps were carried out using a suite of R packages, including nasapower (Sparks, 2018), ggplot2 (Wilkinson et al., 2016), Tidyverse (Wickham et al., 2019), gt (Iannone et al., 2025), sf (Pebesma, 2018; Pebesma & Bivand, 2023), and gstat (Gräler et al., 2016), all within the Quarto environment (Quarto Development Team, 2024).

3. RESULTS

3.1. Characterization of the Observational and Modeled Precipitation Data

Figure 3 presents boxplots of monthly precipitation for each station over the entire observation period. Although these visualizations do not capture seasonal variability, the plots reveal the varying precipitation regimes across different stations. Furthermore, two classification approaches were applied: one based on mean precipitation and another on the Coefficient of Variation (CV), providing complementary perspectives on both the central tendency and dispersion of precipitation data at each location.

Table 1 and Table 2 (appendix) provides complementary monthly statistics, presenting mean and coefficient of variation (CV) in the format ‘mean (CV)’ for each station. The values are separated by a dash (-), with the first corresponding to DGRE observed data and the second to NASA POWER modelled estimates.

Figure 4 presents the spatial distribution of mean annual precipitation for both observed (DGRE) and modelled (NASA POWER) data, along with their corresponding standard deviations. The mapping was generated using an automated iterative kriging procedure that evaluated sixteen variogram models, including Exponential, Spherical, Gaussian, and others, retaining only the best-performing model for each interpolation. The selected model and cross-validation performance metrics are indicated at the bottom of each map.

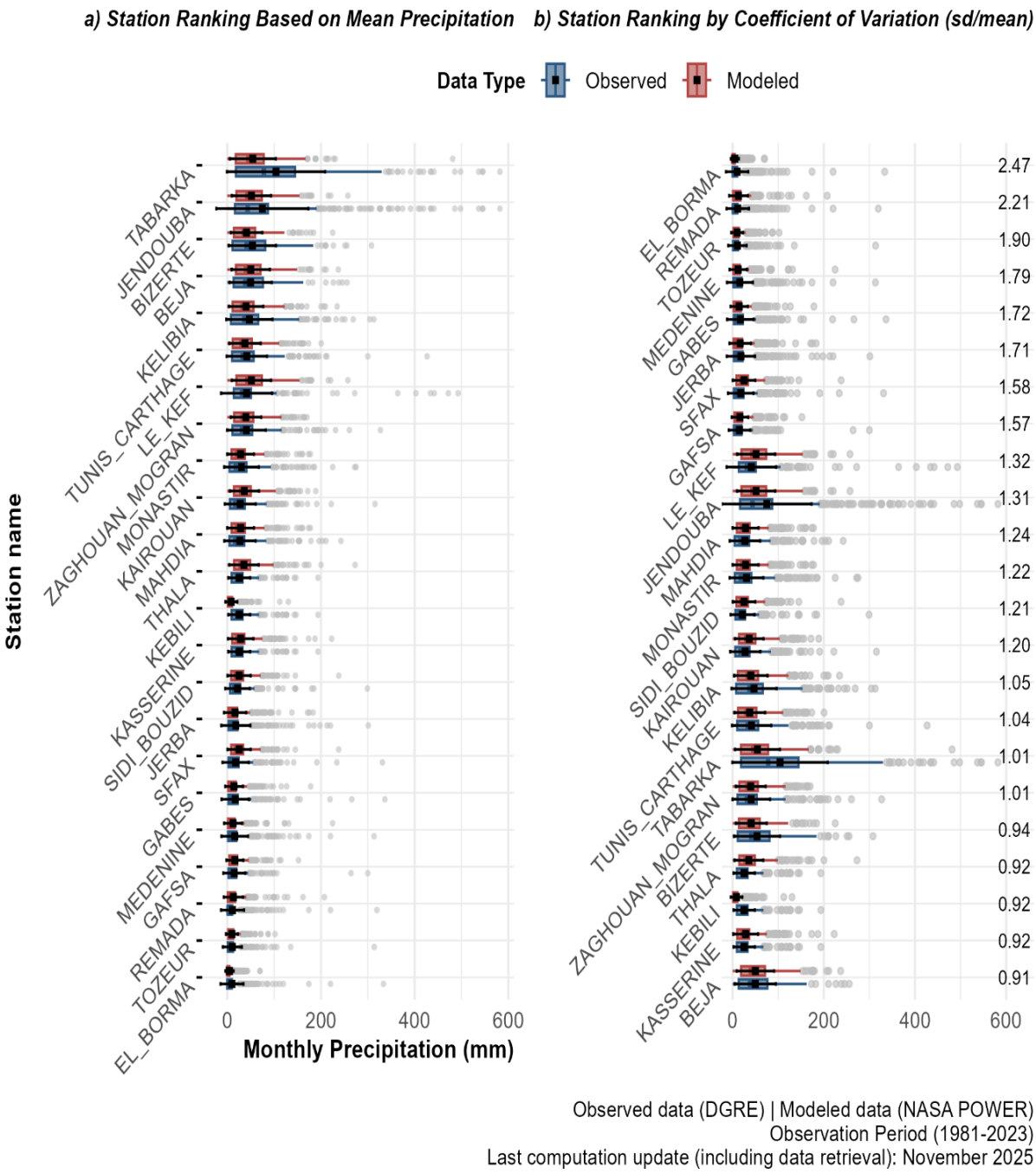

Figure 3. Comparison of monthly observed and modeled precipitation by station.

3.2. Regression results

Figure 5. presents the outcomes of four global regression methods applied to all monthly observed and modelled precipitation data, without stratification by station or month, along with their respective equations and performance metrics.

Figure 6 presents the station-wise regression outcomes for monthly precipitation, accompanied by the automated selection of the optimal model based on their respective R^2 values.

Figure 7 presents the performance of the no-intercept linear model across stations and months. The selection of this model was predicated on its demonstrated superiority in 241 out of 275 cases, as evidenced by its outperformance of the LOESS method. This choice was made with the objective of maintaining methodological consistency with the preceding comments

4. DISCUSSION

The comparative regression analysis demonstrates that the linear model without an intercept

Table 1. Monthly precipitation statistics (January–June)

Station	January	February	March	April	May	June
BEJA	82 (61) – 83 (55)	73 (65) – 60 (75)	62 (50) – 69 (57)	59 (70) – 52 (68)	29 (63) – 43 (67)	18 (125) – 20 (94)
BIZERTE	89 (53) – 55 (63)	81 (63) – 44 (70)	60 (61) – 53 (63)	55 (69) – 46 (71)	25 (65) – 37 (72)	13 (109) – 19 (110)
EL_BORMA	14 (149) – 7 (179)	8 (133) – 6 (159)	15 (125) – 10 (120)	10 (142) – 4 (138)	6 (182) – 5 (266)	1 (127) – 1 (213)
GABES	26 (145) – 19 (168)	10 (83) – 12 (108)	20 (98) – 19 (83)	21 (118) – 13 (91)	12 (133) – 9 (115)	4 (166) – 3 (116)
GAFSA	24 (181) – 22 (161)	9 (80) – 12 (103)	18 (86) – 22 (74)	19 (90) – 19 (81)	13 (79) – 17 (87)	7 (174) – 8 (96)
JENDOUBA	122 (109) – 84 (53)	115 (111) – 62 (74)	113 (110) – 71 (56)	87 (118) – 54 (69)	51 (93) – 46 (67)	31 (127) – 21 (96)
JERBA	29 (122) – 22 (145)	15 (92) – 16 (95)	18 (98) – 21 (96)	13 (102) – 12 (90)	6 (101) – 8 (134)	2 (103) – 3 (162)
KAIROUAN	34 (122) – 48 (94)	20 (99) – 32 (78)	30 (97) – 51 (68)	33 (95) – 38 (64)	28 (95) – 36 (65)	14 (148) – 20 (91)
KASSERINE	27 (137) – 34 (141)	19 (89) – 21 (86)	27 (86) – 41 (82)	33 (72) – 29 (67)	32 (73) – 36 (71)	20 (71) – 21 (75)
KEBILI	27 (137) – 13 (201)	19 (89) – 7 (129)	27 (86) – 11 (85)	33 (72) – 10 (119)	32 (73) – 6 (118)	20 (71) – 3 (151)
KELIBIA	80 (61) – 55 (73)	60 (78) – 44 (65)	52 (64) – 44 (65)	45 (84) – 36 (63)	23 (86) – 24 (81)	10 (126) – 11 (114)
LE_KEF	56 (93) – 84 (53)	50 (151) – 62 (74)	58 (121) – 71 (56)	41 (69) – 54 (69)	48 (142) – 46 (67)	24 (90) – 21 (96)
MAHDIA	40 (101) – 31 (122)	27 (87) – 21 (76)	26 (70) – 35 (68)	21 (64) – 27 (63)	16 (91) – 27 (79)	6 (183) – 13 (107)
MEDENINE	25 (120) – 15 (157)	14 (94) – 13 (93)	21 (99) – 16 (98)	13 (106) – 12 (109)	6 (98) – 10 (128)	2 (157) – 4 (182)
MONASTIR	46 (103) – 31 (122)	27 (87) – 21 (76)	32 (95) – 35 (68)	25 (57) – 27 (63)	18 (92) – 27 (79)	7 (125) – 13 (107)
REMADA	16 (145) – 16 (138)	11 (127) – 16 (97)	16 (111) – 18 (108)	9 (140) – 11 (111)	6 (146) – 11 (172)	2 (93) – 3 (151)
SFAX	25 (147) – 29 (150)	12 (117) – 20 (88)	22 (98) – 36 (70)	19 (97) – 25 (61)	14 (105) – 24 (69)	5 (158) – 13 (90)
SIDI_BOUZID	31 (138) – 29 (150)	14 (94) – 20 (88)	26 (85) – 36 (70)	28 (93) – 25 (61)	23 (86) – 24 (69)	11 (100) – 13 (90)
TABARKA	179 (67) – 92 (51)	157 (75) – 71 (74)	137 (84) – 67 (57)	112 (87) – 55 (66)	56 (81) – 40 (76)	29 (142) – 17 (104)
THALA	27 (137) – 47 (112)	19 (89) – 30 (82)	27 (86) – 52 (76)	33 (72) – 36 (64)	32 (73) – 36 (62)	20 (71) – 23 (84)
TOZEUR	17 (156) – 15 (170)	6 (92) – 8 (118)	12 (105) – 14 (85)	16 (109) – 12 (91)	9 (107) – 9 (96)	5 (228) – 4 (122)
TUNIS_CARTHAGE	65 (60) – 50 (70)	54 (66) – 40 (68)	43 (57) – 45 (68)	46 (78) – 38 (68)	24 (72) – 28 (76)	15 (125) – 15 (124)
ZAGHOUAN_MOGRAN	73 (93) – 54 (75)	47 (73) – 39 (76)	47 (60) – 54 (64)	47 (77) – 43 (69)	27 (71) – 39 (67)	12 (112) – 21 (100)

CV = coefficient of variation (%). Observed – modeled. Format: mean (CV). Data source: Observed (DGRE), Modeled (NASA POWER). Period of observation: 1981–2023. Last download: November 2025.

CV = coefficient of variation (%). Observed – modeled. Format: mean (CV). Data source: Observed (DGRE), Modeled (NASA POWER). Period of observation: 1981–2023. Last download: November 2025.

Table 2. Monthly precipitation statistics (July–December)

Station	July	August	September	October	November	December
BEJA	5 (158) – 7 (111)	12 (198) – 19 (90)	40 (64) – 46 (61)	60 (77) – 56 (57)	73 (69) – 68 (59)	82 (54) – 77 (60)
BIZERTE	4 (155) – 6 (122)	6 (187) – 18 (112)	44 (83) – 49 (65)	65 (67) – 54 (58)	90 (48) – 52 (55)	111 (53) – 60 (69)
EL_BORMA	1 (151) – 0 (284)	9 (574) – 0 (187)	4 (152) – 3 (136)	16 (171) – 7 (153)	11 (131) – 6 (125)	23 (195) – 8 (111)
GABES	2 (288) – 1 (122)	10 (515) – 5 (102)	23 (134) – 21 (93)	29 (159) – 24 (112)	22 (112) – 21 (90)	26 (87) – 23 (89)
GAFSA	2 (139) – 3 (107)	12 (370) – 9 (103)	19 (101) – 22 (68)	19 (112) – 19 (72)	20 (103) – 20 (98)	16 (92) – 20 (109)
JENDOUBA	9 (161) – 7 (116)	20 (222) – 20 (89)	53 (93) – 48 (61)	75 (99) – 57 (56)	89 (89) – 68 (61)	132 (101) – 79 (61)
JERBA	1 (140) – 1 (144)	9 (522) – 4 (147)	15 (160) – 21 (108)	36 (126) – 30 (134)	27 (99) – 29 (95)	48 (95) – 33 (83)
KAIROUAN	5 (136) – 7 (103)	19 (255) – 21 (99)	44 (95) – 49 (68)	45 (70) – 50 (59)	32 (91) – 41 (64)	27 (97) – 44 (79)
KASSERINE	13 (103) – 9 (87)	23 (95) – 21 (91)	38 (76) – 36 (55)	27 (62) – 32 (61)	26 (106) – 32 (93)	21 (71) – 31 (112)
KEBILI	13 (103) – 1 (170)	23 (95) – 2 (121)	38 (76) – 11 (99)	27 (62) – 13 (111)	26 (106) – 11 (91)	21 (71) – 13 (106)
KELIBIA	6 (227) – 5 (130)	12 (398) – 15 (130)	43 (69) – 56 (75)	82 (84) – 68 (60)	73 (71) – 57 (66)	80 (60) – 64 (61)
LE_KEF	8 (133) – 7 (116)	22 (254) – 20 (89)	37 (72) – 48 (61)	40 (88) – 57 (56)	61 (142) – 68 (61)	49 (81) – 79 (61)
MAHDIA	1 (134) – 5 (132)	6 (208) – 17 (120)	39 (125) – 49 (84)	52 (81) – 48 (62)	40 (99) – 33 (80)	48 (81) – 34 (98)
MEDENINE	1 (131) – 1 (204)	9 (538) – 2 (129)	12 (143) – 14 (100)	25 (141) – 20 (139)	24 (125) – 20 (176)	39 (117) – 20 (96)
MONASTIR	3 (151) – 5 (132)	15 (287) – 17 (120)	44 (103) – 49 (84)	58 (89) – 48 (62)	41 (81) – 33 (80)	46 (82) – 34 (98)
REMADA	1 (150) – 0 (174)	9 (565) – 2 (177)	6 (112) – 13 (121)	17 (168) – 23 (150)	14 (113) – 20 (166)	27 (165) – 22 (84)
SFAX	2 (155) – 6 (111)	12 (406) – 17 (101)	20 (132) – 38 (70)	34 (127) – 35 (66)	23 (110) – 30 (84)	24 (81) – 29 (96)
SIDI_BOUZID	6 (113) – 6 (111)	22 (208) – 17 (101)	32 (96) – 38 (70)	27 (67) – 35 (66)	20 (88) – 30 (84)	19 (84) – 29 (96)
TABARKA	7 (131) – 5 (108)	19 (249) – 16 (105)	68 (77) – 44 (60)	111 (67) – 60 (58)	165 (43) – 85 (51)	210 (54) – 101 (76)
THALA	13 (103) – 10 (85)	23 (95) – 24 (92)	38 (76) – 45 (55)	27 (62) – 43 (59)	26 (106) – 40 (83)	21 (71) – 40 (89)
TOZEUR	2 (167) – 1 (132)	11 (450) – 4 (116)	12 (148) – 12 (79)	14 (143) – 12 (86)	13 (107) – 13 (100)	11 (107) – 13 (118)
TUNIS_CARTHAGE	6 (167) – 5 (126)	14 (324) – 15 (125)	49 (138) – 52 (78)	55 (80) – 58 (62)	57 (61) – 50 (67)	72 (69) – 56 (66)
ZAGHOUAN_MOGRAN	5 (167) – 7 (110)	11 (121) – 19 (99)	46 (86) – 50 (68)	61 (75) – 54 (57)	55 (74) – 46 (60)	61 (62) – 52 (68)

CV = coefficient of variation (%). Observed – modeled. Format: mean (CV). Data source: Observed (DGRE), Modeled (NASA POWER). Period of observation: 1981–2023. Last download: November 2025.

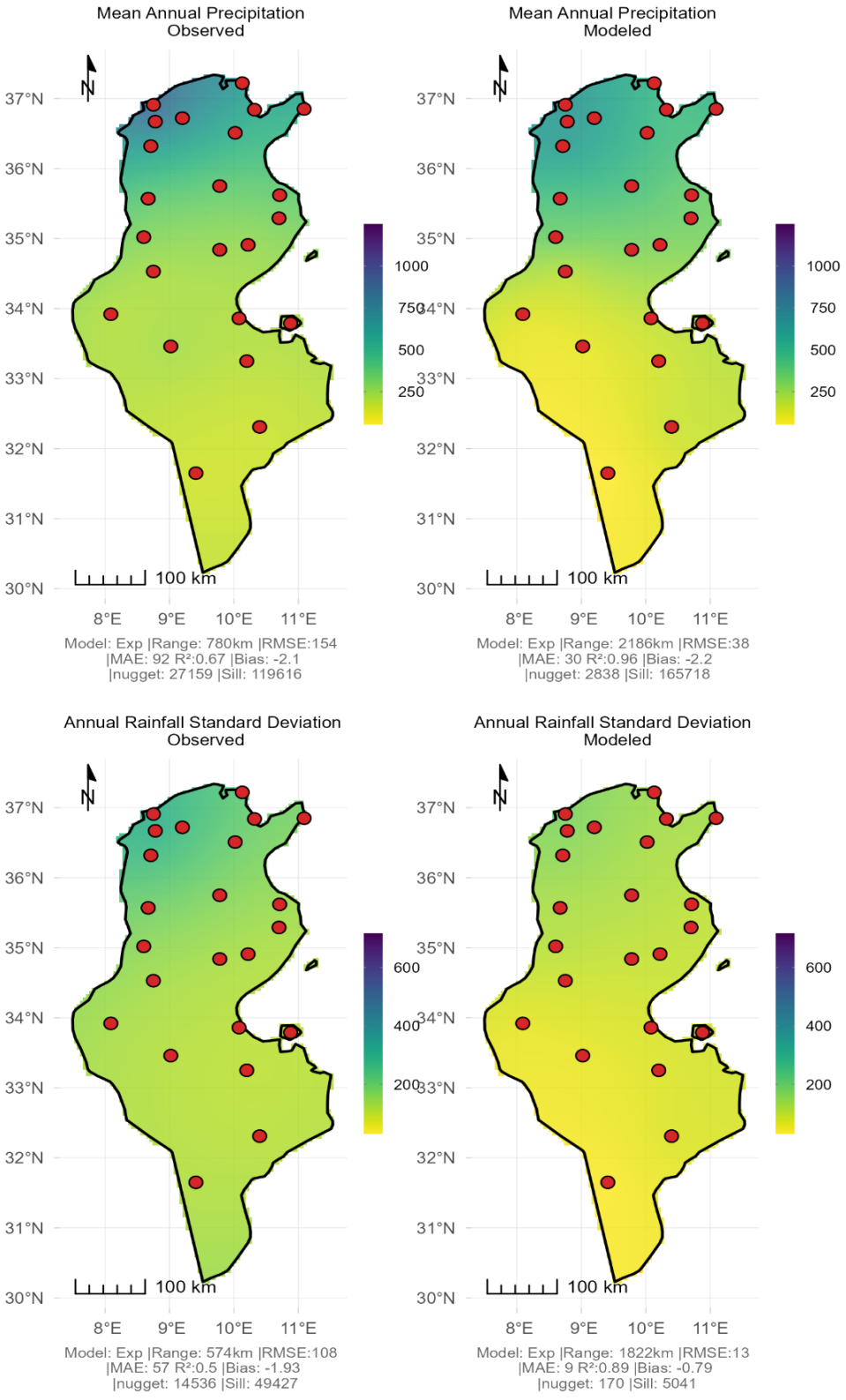

Figure 4. Spatial distribution of annual precipitation.

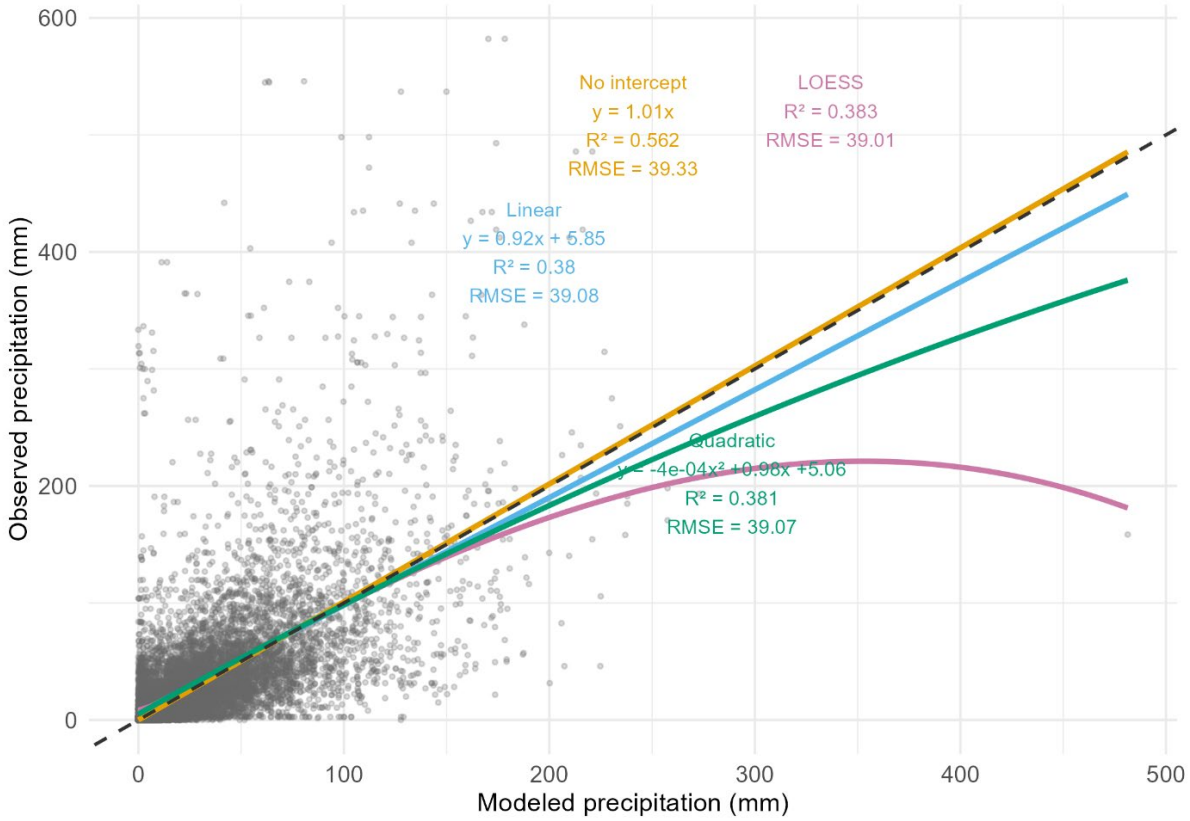

Global regression between observed (DGRE) and modeled (NASA POWER) monthly precipitation data (1981–2023). The figure compares four models—linear, quadratic, exponential, and LOESS—showing their respective equations, coefficients of determination (R^2), and root mean square error (RMSE) values. The linear model without intercept provided the best fit (R^2 = 0.562; RMSE = 39.0 mm), confirming its suitability for large-scale evaluation.

Figure 5. Global regression between observed (DGRE) and modeled (NASA POWER) monthly precipitation data (1981-2023).

($y = 1.01x$) yields the optimal fit, attaining a coefficient of determination (R^2) of 0.562 and a root mean square error (RMSE) of 39.0 mm (Figure 5). On a global scale, this performance falls within the typical range ($R^2 \approx 0.4$ l)- 0.60 reported in recent studies evaluating modelled or satellite-derived precipitation against in situ gauge observations at monthly resolution (Monteiro et al., 2018; Wei et al., 2018). "Model performances with $NSE > 0.5$ (which corresponds roughly to $R^2 > 0.5$) when the model is unbiased are considered acceptable" (Gupta et al., 2009). The absence of a statistically significant intercept indicates that there is no systematic offset bias, which supports the reliability of the model for large-scale applications. On a global scale, the NASA POWER monthly precipitation dataset, when compared against the complete network of reference stations, achieves a coefficient of determination of approximately $R^2 \approx 0.61$ and an RMSE of 61 mm (linear fit: y = 0.67x + 30.08; (*NASA POWER | Prediction Of Worldwide Energy Resources*, 2025)). These metrics seem higher than those obtained in the present results (Figure 5). However, they should be interpreted with caution, as the project's methodological documentation (NASA POWER, Precipitation Methodology) shows considerable scatter in the data, with the linear fit masking substantial spatiotemporal variability. By aggregating data at the global scale, regional, seasonal, and climate-regime-specific biases are partially mitigated. The subsequent analysis therefore investigates these variabilities in detail, considering each station, and month, in order to uncover the sources of discrepancies and propose targeted ways to improve the dataset.

Figure 4 illustrates the model's representation of spatial variability when monthly precipitation is aggregated to the annual timescale. By comparing maps of annual mean and standard deviation between observed (DGRE) and modeled (NASA POWER) precipitation, it is clear that the model reproduces the large-scale spatial patterns of mean annual rainfall very well (R^2 = 0.96), with almost no bias. The model, however, has two notable limitations. Firstly, extreme precipitation values are systematically underestimated, particularly in the northwestern orographic zones. Observed annual totals can surpass 1000 mm, while the model rarely exceeds 750 mm, highlighting the limitations of its ~50 km spatial resolution in capturing fine-scale terrain variations. Secondly, the model underrepresents interannual variability.

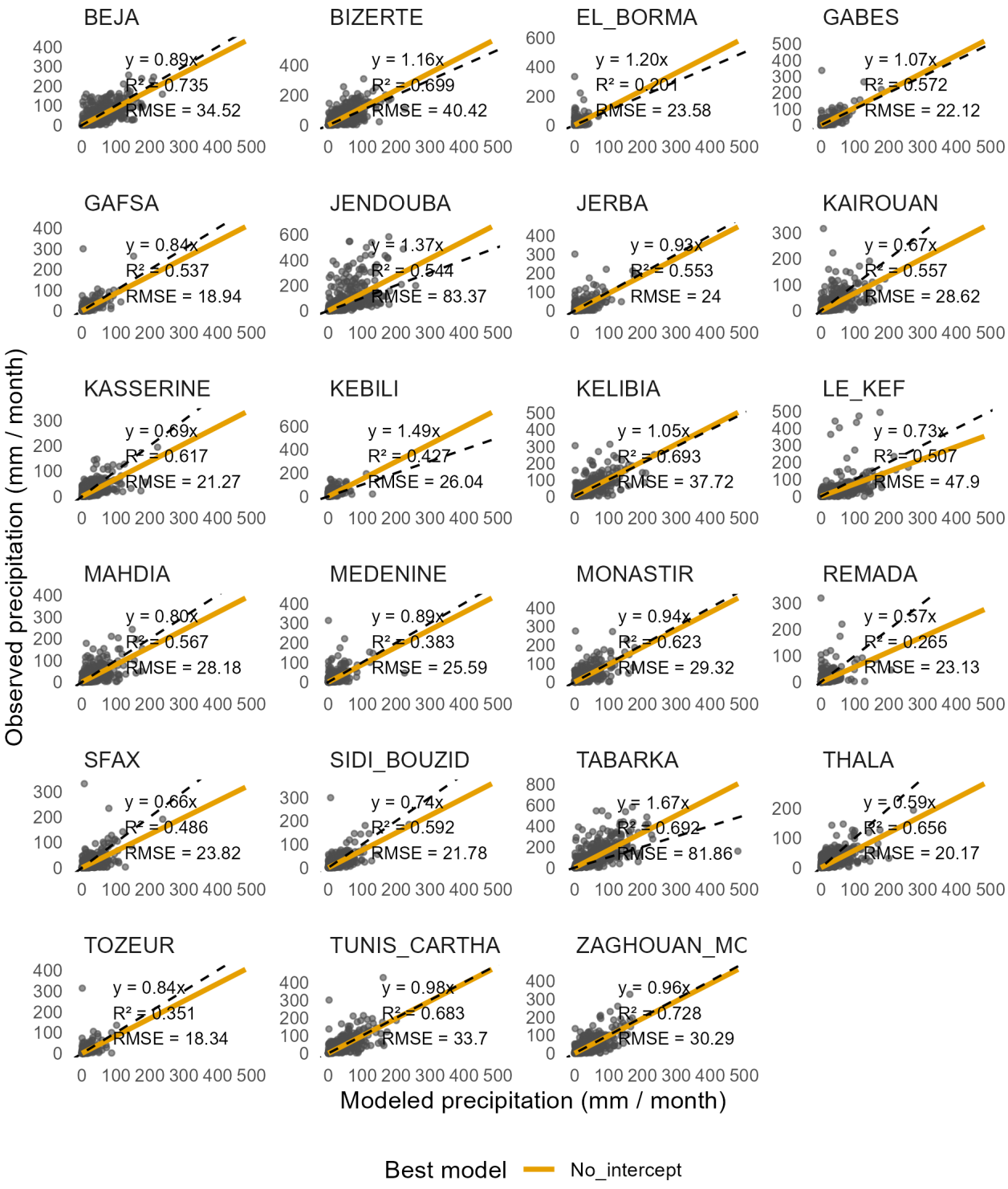

--- reference : y = x. Modeled data: NASA POWER. Observed data: DGRE.
Observation period: 1981–2023. Last data download: November 2025

Station-by-station regression analyses comparing observed (DGRE)and modeled (NASA POWER) monthly precipitation the period 1981–2023.The optimal regression model for each station was selected based on the highest R^2 value among linear, quadratic, and exponential models.Slopes below 1 indicate underestimation of high rainfall in norther nregions (e.g., BEJA, GAFSA), while slopes above 1 indicate overestimation of light rainfall in southern stations (e.g., KEBILI, EL BORMA).

Figure 6. Regression analysis per station.

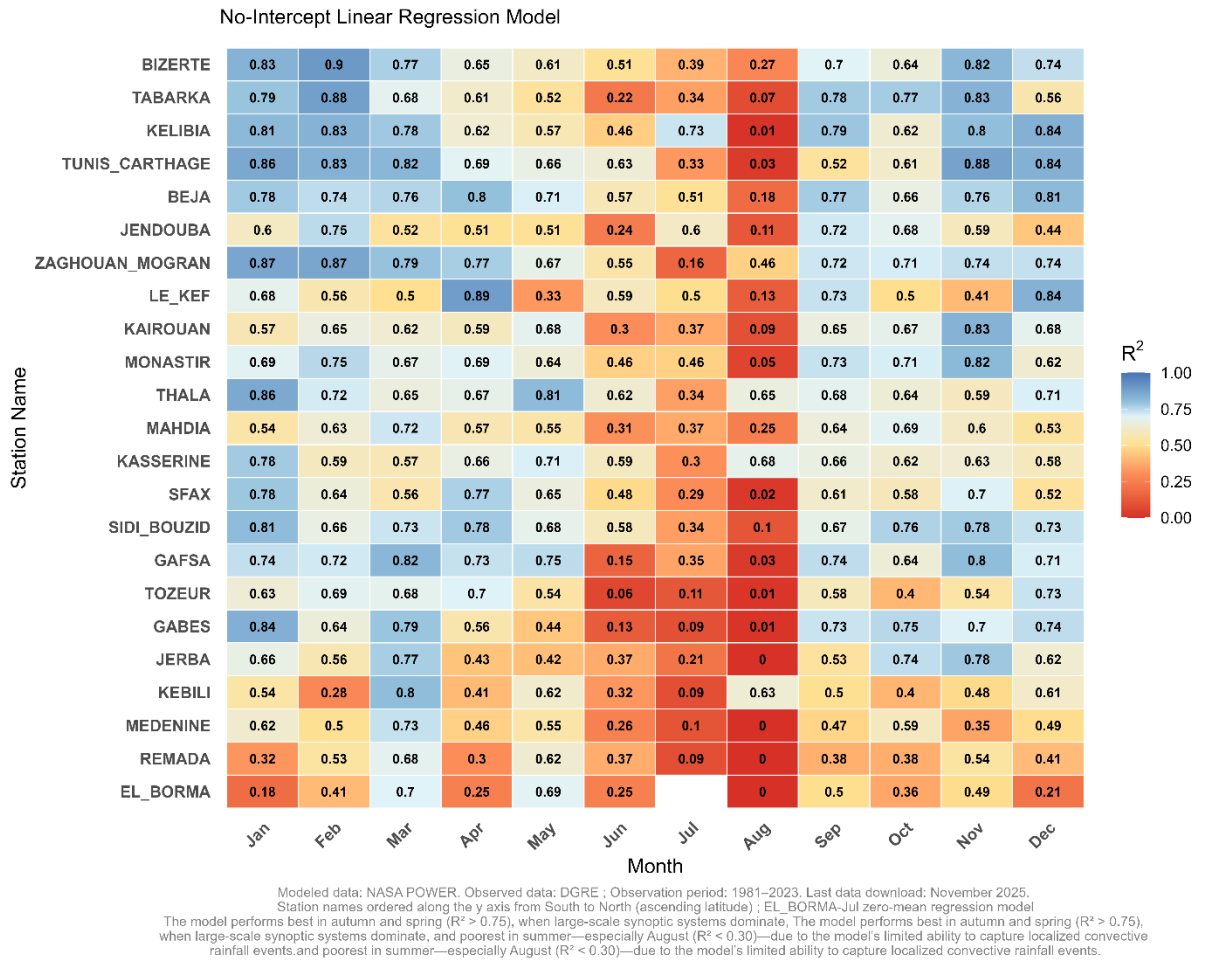

Figure 7. Regression analysis by station and month.

Although the spatial correlation remains high (R^2 = 0.89), the modeled annual standard deviation falls short by almost 30% in highly variable regions, decreasing from 600 mm to 400 mm. This indicates that the model preserves the overall spatial structure but underestimates the true amplitude of interannual variability, probably due to MERRA-2's parameterization choices, which emphasize stability at the global scale rather than fine-scale climatic fluctuations. His limitation is particularly evident in Tunisia, where precipitation exhibits pronounced spatiotemporal contrasts (Fathalli et al., 2019), with annual totals ranging from over 1600 mm in the north to less than 50 mm in the south, coupled with strong seasonality. Across a distance of only ~600 km, the country transitions from humid and sub-humid climates to hyper-arid Saharan conditions, forming a complex climatic mosaic. Under such conditions, high-resolution representation of both mean precipitation and variability is essential, yet the current model is unable to fully capture these patterns. This complexity reflects a common challenge in Mediterranean hydro-climatology. As shown by EL-HAMDOUNY et al. (2025) in Morocco, rainfall series in data-scarce basins require rigorous quality assessments to filter unreliable data that can distort regional patterns.

A station-by-station assessment was performed to evaluate NASA POWER precipitation data. Results show variations in performance linked to the local climate. The DGRE network, shown in Figure 2, extends from the north to the south, allowing examination of the model across areas with different rainfall characteristics. The boxplots in Figure 3 indicate that the model behaves differently depending on station location. In the north, median monthly values are approximated, but extreme months are underestimated, with observed maxima exceeding 500 mm while modeled values remain around 400–450 mm. In the south, where the coefficient of variation is higher, the model compresses interannual variability, limiting the representation of unusually dry or wet years.

Figure 6 illustrates how regression slopes differ among stations. In northern and central stations such as BEJA (0.89) and GAFSA (0.84), slopes below 1 indicate that high rainfall is underestimated. In southern stations like KEBILI (1.49) and EL-

BORMA (1.20), slopes above 1 show that lighter rainfall is overestimated. Coefficients of determination range from 0.20 to 0.74, highlighting the model's limitations in reproducing local precipitation patterns under variable topography and climate.

Figure 7 shows that the model performs best in autumn and spring, when R^2 values exceed 0.75. During these seasons, rainfall is mainly driven by large-scale frontal systems that the model represents well. In contrast, performance decreases in summer, especially in July and August, and to a lesser extent in winter. These drops are not uniform across the country but vary from one region to another.

In the northern stations such as TABARKA, Bizerte, and LE KEF, the model keeps R^2 values above 0.70 during most months. The main exception is August, when R^2 drops to about 0.59–0.77. This month shows very large year-to-year variability in the observations, with coefficients of variation above 240%, linked to irregular summer storms. The model reduces this variability to around 90–105%.

Along the coast, at sites like KELIBIA, Mahdia, and Monastir, performance is generally maintained in winter and spring. However, August again stands out as a weak point. For example, at KELIBIA the observed CV reaches nearly 400%, while the model gives about 130%; at Mahdia, the observed value is around 208% compared to 120% in the model. This shows that even in coastal areas, summer variability is not well represented

In the central stations such as KAIROUAN, SIDI BOUZID, and KASSERINE, the model shows lower agreement with observations. During autumn and spring, R^2 values range between about 0.40 and 0.65, but in August, they drop below 0.30. At KAIROUAN, the observed coefficient of variation in August reaches 255%, while the model gives only about 99%, showing that rare but intense summer rainfall events are not captured. This seasonal accuracy relates to observations by ZHANG et al. (2017) in China, where the correlation between dry-wet climatic factors and environmental responses depends on the precision of intra-annual variability and seasonal precipitation indices.

In the Saharan stations of EL-BORMA, KEBILI, and TOZEUR, R^2 values remain below 0.30 throughout the year, indicating low correspondence between observed and modeled precipitation. During summer, observed interannual variability is extremely high, with CVs reaching 574% at EL-BORMA and 450% at TOZEUR in August. The model, however, shows very little variability or overly smoothed values. At EL-BORMA in July, the regression failed entirely, producing a constant model ($y = 0$) because no linear relationship could be identified between observations and model outputs. The limitation of the model in Saharan and arid stations aligns with observations in other Eastern Mediterranean contexts. ÇİÇEK & DUMAN (2015) highlighted in Turkey that while northern regions may show different precipitation patterns, southern semi-arid regions face increasing aridity risks that global models struggle to quantify accurately.

It is important to note that August is not the only problematic month. It has been demonstrated that certain central stations (e.g., LE KEF, KAIROUAN) demonstrate poorly captured high variability during the winter months. For instance, at LE KEF in January, the observed CV is 93% compared to 53% in the model. As indicated by the falling R^2 values observed in June, a transitional month marking the onset of the dry season, difficulties in representing the end of the rainy season are indicated at several stations (JENDOUBA: 0.24; SIDI BOUZID: 0.28).

The observed discrepancies in variability relate to environmental monitoring challenges. As shown by Rabah MAYOUF & Mohamed Tahar HANAFI (2025) in Algeria, the effectiveness of drought indices remains dependent on the accurate representation of precipitation inputs in Mediterranean ecosystems.

In summary, NASA POWER reproduces precipitation well during periods influenced by large-scale synoptic systems, particularly in autumn and spring. During seasons with irregular and localized rainfall, such as summer, the model underestimates interannual variability. This behavior reflects a structural limitation: the model's coarse spatial resolution cannot capture local convective processes. The issue occurs across all stations and months, not at specific locations.

The irregular rainfall observed in KAIROUAN during August, December, and January has also been reproduced using a stochastic rainfall generator based on a Markov chain. This approach captures the patterns of rainfall occurrence and intensity typical of these months in a semi-arid climate (Mouelhi et al., 2016).

In view of the systematic underestimation of interannual variability (particularly during the summer months, and most notably in August, "a missing piece in the precipitation modeling puzzle for semi-arid regions) a promising avenue for future work lies in the adoption of hierarchical Bayesian frameworks that explicitly model dispersion metrics such as the coefficient of variation (CV). Rather than regarding variability as residual noise, such approaches treat it as a structured, spatially correlated process. This enables more realistic probabilistic

reconstructions of precipitation fields in complex Mediterranean and semi-arid environments.

Consequently, it is recommended to use NASA POWER data with caution for local hydrological modeling in arid zones. Ground-based observations are essential for correcting the underestimation of intra-annual variability in environmental monitoring. Finally, regional bias-correction factors should be developed for transition months to improve the reliability of satellite-based products for water management.

5. CONCLUSION

The present study conducted a comprehensive station-by-station and month-by-month evaluation of NASA POWER monthly precipitation estimates against ground-based observations from 23 meteorological stations distributed across Tunisia's entire climatic gradient, from the humid north to the Saharan south, over the period 1981–2023.

NASA POWER successfully reproduces the broad north–south gradient and large-scale spatial pattern of mean annual precipitation (spatial R^2 = 0.96), yet it systematically underestimates orographic extremes in the northwest (observed > 1 000 mm yr^{-1} at TABARKA versus < 750 mm yr^{-1} modelled) and, more importantly, strongly dampens interannual and monthly variability across the country. This attenuation reaches approximately 30 % for annual standard deviation in the most variable regions and becomes particularly severe at the monthly scale, most notably in August, when observed coefficients of variation regularly exceed 250 % in central Tunisia (e.g., 255 % at KAIROUAN) and 500 % in the south (e.g., 574 % at EL BORMA), whereas the model returns values as low as 99 % or near zero. This underestimation reflects the dataset's inability to represent localized, high-intensity convective events that control summer rainfall and cause the large interannual variability typical of Mediterranean and semi-arid climates.

Model performance is satisfactory during autumn (October–December) and spring (March–April). Large-scale frontal systems prevail during these months (R^2 > 0.70 in most northern stations). However, model performance deteriorates during summer. This is especially the case in August (R^2 < 0.30 in central and southern regions). There is also a moderate decline in certain winter and transitional months at individual stations. These limitations are linked to the product's spatial resolution of about 50 km, which is not sufficient to capture the small-scale convective processes that drive precipitation variability in Tunisia.

As a result, the NASA POWER precipitation dataset cannot be directly used for hydrological modeling, agricultural planning, or water-resource management in Tunisia without applying bias corrections specific to each station and month. Accurate representation of both mean rainfall and interannual variability, especially the irregularity observed in August, is essential for these applications.

Future research should focus on developing hybrid products or hierarchical Bayesian approaches that treat the coefficient of variation as a structured, spatially consistent process rather than as random noise. In addition, stochastic downscaling methods are needed to reproduce the high variability observed in summer and transitional months in semi-arid regions. This study highlights the importance of local validation before using global gridded precipitation datasets for operational applications in areas with strong climatic variability and localized convective rainfall.

Author contribution statement

All authors contributed equally to the conception, design, analysis, and writing of this manuscript.

REFERENCES

Aboelkhair, H., Morsy, M., & El Afandi, G. (2019). *Assessment of agroclimatology NASA POWER reanalysis datasets for temperature types and relative humidity at 2 m against ground observations over Egypt*. Advances in Space Research, 64(1), 129–142. https://doi.org/10.1016/j.asr.2019.03.032

Abubakar, I. M., & Idi, B. Y. (2024). *Statistical analysis of NASA POWER meteorological data for the assessment of climate variability in Adamawa State*. Environmental Technology and Science Journal, *15*(2), Article 2. https://doi.org/10.4314/etsj.v15i2.13

Asilevi, P. J., Dogbey, F., Boakye, P., Aryee, J. N. A., Yamba, E. I., Owusu, S. Y., Peprah, D. K., Quansah, E., Klutse, N. A. B., Bentum, J. K., Adjei, K. A., Anornu, G. K., Oduro-Kwarteng, S., & Amekudzi, L. K. (2024). *Bias-corrected NASA data for aridity index estimation over tropical climates in Ghana, West Africa*. Journal of Hydrology: Regional Studies, 51, 101610. https://doi.org/10.1016/j.ejrh.2023.101610

Bargaoui, Z., Tramblay, Y., Lawin, E. A., & Servat, E. (2014). *Seasonal precipitation variability in regional climate simulations over Northern basins of Tunisia: Regional Climate Simulations of Precipitation Over North Tunisia*. International Journal of Climatology, 34(1), 235–248. https://doi.org/10.1002/joc.3683

Bell, V. A., & Moore, R. J. (2000). *The sensitivity of*

catchment runoff models to rainfall data at different spatial scales. Hydrology and Earth System Sciences, 4(4), 653–667. https://doi.org/10.5194/hess-4-653-2000

Ben Othman, A., Ouni, A., & Besbes, M. (2020). *Deep learning-based estimation of PV power plant potential under climate change: A case study of El Akarit, Tunisia.* Energy, Sustainability and Society, 10(1), 34. https://doi.org/10.1186/s13705-020-00266-1

Bensefia, S., Kouider, D. B., & Athmani, H. (2026). *Assessment of sand encroachment in arid regions: A case study of el hajeb municipality, biskra province, southeastern sahara, algeria.* Carpathian Journal of Earth and Environmental Sciences, 21(1), 35–48. https://doi.org/10.26471/cjees/2026/021/350

Bivand, R. S., Pebesma, E., & Gómez-Rubio, V. (2013). *Applied Spatial Data Analysis with R*. Springer. https://doi.org/10.1007/978-1-4614-7618-4

Burnham, K. P., & Anderson, D. R. (2002). *Model selection and multimodel inference: A practical information-theoretic approach*. Springer Verlag.

Célestin, M., Emmanuel, L. A., Batablinlè, L., & Marc, N. (2019). *Spatio-Temporal Analysis of Climate Change Impact on Future Wind Power Potential in Burundi (East Africa)*. American Journal of Climate Change, 8(2), Article 2. https://doi.org/10.4236/ajcc.2019.82014

Chiew, F. H., Jones, R. N., & Boughton, W. C. (2005). *Modelling hydrologic sensitivity to climate conditions*. In 29th hydrology and water resources symposium: Water capital, 20-23 february 2005, rydges lakeside, canberra. Engineers Australia. https://search.informit.org/doi/10.3316/informit.976268249630759

Çiçek, İ., & Duman, N. *(2015). Seasonal and annual precipitation trends in Turkey. C*arpathian Journal of Earth and Environmental Sciences, 10(2), 77–84.

Dawa, S. Y., Tan, M. L., Samat, N., Roy, R., & Zhang, F. (2024). *Evaluation of five gridded precipitation products for estimating precipitation and drought over Yobe, Nigeria*. Water Supply, 24(6), 2039–2054. https://doi.org/10.2166/ws.2024.113

Edwards, P. N., Mayernik, M. S., Batcheller, A. L., Bowker, G. C., & Borgman, C. L. (2011). *Science friction: Data, metadata, and collaboration*. Social Studies of Science, 41(5), 667–690. https://doi.org/10.1177/0306312711413314

El-Hamdouny, M., Garouani, M. E., El-Yazidi, M., Midaoui, A., Goumih, M., & Lahrach, A. (2025). *Data quality assessment and homogenization of rainfall time series in data-scarce regions: A case study of the upper oum er-rbia basin, northern morocco*. Carpathian Journal of Earth and Environmental Sciences, 20(1). https://doi.org/10.26471/cjees/2025/020/317

Farhani, N., Carreau, J., Kassouk, Z., Le Page, M., Lili Chabaane, Z., & Boulet, G. (2022). *Analysis of Multispectral Drought Indices in Central Tunisia*. Remote Sensing, 14(8). https://doi.org/10.3390/rs14081813

Fathalli, B., Pohl, B., Castel, T., & Safi, M. J. (2019). *Errors and uncertainties in regional climate simulations of rainfall variability over Tunisia: A multi-model and multi-member approach*. Climate Dynamics, 52(1), 335–361. https://doi.org/10.1007/s00382-018-4150-2

Ghane, M., Alvankar, S. R., Eslamian, S., Amoushahi-Khouzani, M., Gandomkar, A., Zamani, E., Marani-Barzani, M., Kazemi, M., Soltani, M., Dehghan, S., P.Singh, V., Ostad-Ali-Askari, K., Haeri-Hamedani, M., Shirvani-Dastgerdi, H.-R., Zalaki-Badil, N., Majidifar, Z., R.Dalezios, N., & Soltani, B. (2017). *Sensitivity Analysis of Runoff Model by SWAT to Meteorological Parameters: A Case Study of Kasillian Watershed, Mazandaran, Iran*. International Journal of Research Studies in Agricultural Sciences, 3(10), 17–36. https://www.arcjournals.org/international-journal-of-research-studies-in-agricultural-sciences/volume-3-issue-10/3

Gharnouki, I., Aouissi, J., Benabdallah, S., & Tramblay, Y. (2024). *Assessing the variability of satellite and reanalysis rainfall products over a semiarid catchment in Tunisia.* Acta Geophysica, 72(2), 1257–1273. https://doi.org/10.1007/s11600-024-01293-8

Gräler, B., Pebesma, E., & Heuvelink, G. (2016). *Spatio-Temporal Interpolation using gstat.* The R Journal, 8(1), 204–218. https://journal.r-project.org/archive/2016/RJ-2016-014/index.html

Gupta, H. V., Kling, H., Yilmaz, K. K., & Martinez, G. F. (2009). *Decomposition of the mean squared error and NSE performance criteria: Implications for improving hydrological modelling.* Journal of Hydrology, 377(1), 80–91. https://doi.org/10.1016/j.jhydrol.2009.08.003

Harris, I., Jones, P. d., Osborn, T. j., & Lister, D. h. (2014). *Updated high-resolution grids of monthly climatic observations – the CRU TS3.10 Dataset. I*nternational Journal of Climatology, 34(3), 623–642. https://doi.org/10.1002/joc.3711

Hersbach, H., Bell, B., Berrisford, P., Biavati, G., Horányi, A., Muñoz Sabater, J., Nicolas, J., Peubey, C., Radu, R., Rozum, I., Schepers, D., Simmons, A., Soci, C., Dee, D., & Thépaut, J.-N. (2023). E*RA5 hourly data on single levels from 1940 to present. Copernicus Climate Change Service (C3S)* Climate Data Store (CDS). Copernicus Climate Change Service (C3S) Climate Data Store (CDS). https://doi.org/10.24381/cds.adbb2d47

Hohmann, C., Kirchengast, G., O, S., Rieger, W., & Foelsche, U. (2020). *Runoff sensitivity to spatial rainfall variability: A hydrological modeling study with dense rain gauge observations.* Hydrology and Earth System Sciences Discussions, 1–28. https://doi.org/10.5194/hess-2020-453

Iannone, R., Cheng, J., Schloerke, B., Hughes, E.,

Lauer, A., Seo, J., Brevoort, K., & Roy, O. (2025). *gt: Easily create presentation-ready display tables* [Manual]. https://gt.rstudio.com

Jiménez-Jiménez, S. I., Ojeda-Bustamante, W., Inzunza-Ibarra, M. A., & Marcial-Pablo, M. de J. (2021). *Analysis of the NASA-POWER system for estimating reference evapotranspiration in the Comarca Lagunera, Mexico.* Revista Chapingo Serie Horticultura, 13(2). https://doi.org/10.5154/r.inagbi.2021.03.050

Jing, X., Leigh, L., Pinto, C. T., & Helder, D. (2019). *Evaluation of RadCalNet Output Data Using Landsat 7, Landsat 8, Sentinel 2A, and Sentinel 2B Sensors*. https://ntrs.nasa.gov/citations/20642178218907

Kadhim Tayyeh, H., & Mohammed, R. (2023). *Analysis of NASA POWER reanalysis products to predict temperature and precipitation in Euphrates River basin.* Journal of Hydrology, 619,129327. https://doi.org/10.1016/j.jhydrol.2023.129327

Kheyruri, Y., & Sharafati, A. (2022). *Spatiotemporal Assessment of the NASA POWER Satellite Precipitation Product over Different Regions of Iran.* Pure and Applied Geophysics, 179(9), 3427–3439. https://doi.org/10.1007/s00024-022-03133-6

Latiri, K., Lhomme, J. P., Annabi, M., & Setter, T. L. (2010). W*heat production in Tunisia: Progress, inter-annual variability and relation to rainfall.* European Journal of Agronomy, 33(1),33–42. https://doi.org/10.1016/j.eja.2010.02.004

Liu, P., Liang, Z., Qian, M., Hu, Y., Wang, J., & Li, B. (2024). A*nalysis of flood streamflow sensitivity to precipitation using the WRF-Hydro model in a humid environment.* Hydrology Research, 55(7), 728–748. https://doi.org/10.2166/nh.2024.011

Matallah, M. E., Matzarakis, A., Boulkaibet, A., Ahriz, A., Zitouni, D. C., Ben Ratmia, F. Z., Mahar, W. A., Ghanemi, F., & Attia, S. (2025). *Refining climate zoning in North Africa: A 30-Year analysis of heating and cooling degree days for energy planning and adaptation.* Energy and Buildings, *342*, 115852. https://doi.org/10.1016/j.enbuild.2025.115852

MAWRF. (2022). *Development of the vision and strategy for the water sector in tunisia by 2050* [Technical report]. Ministry of Agriculture, Water Ressources and Fisheries, Tunisia. http://www.onagri.nat.tn/uploads/secteur-eau/1.pdf

Rodrigues, M. J., Durre, I., Vose, R. S., Gleason, B. E., & Houston, T. G. (2012). *An Overview of the Global Historical Climatology Network-Daily Database.* Journal of Atmospheric and Oceanic Technology, 29(7), 897–910. https://doi.org/10.1175/JTECH-D-11-00103.1

Monteiro, L. A., Sentelhas, P. C., & Pedra, G. U. (2018). A*ssessment of NASA/POWER satellite-based weather system for Brazilian conditions and its impact on sugarcane yield simulation.* International Journal of Climatology, 38(3), 1571–1581. https://doi.org/10.1002/joc.5282

Mouelhi, S., Kanzari, S., Ben Mariem, S., & Zemni, N. (2025). *Towards a Classification of Tunisian Dams for Enhanced Water Scarcity Governance: Parametric or Non-Parametric Approaches?* Hydrology, 12(4), Article 4. https://doi.org/10.3390/hydrology12040096

Mouelhi, S., Nermi, S., Jebari, S., & Slimani, M. (2016). *Using the Markov Chain for the Generation of Monthly Rainfall Series in a Semi-Arid Zone*. Open Journal of Modern Hydrology, 6(2), 51–65. https://doi.org/10.4236/ojmh.2016.62006

NASA POWER | Prediction Of Worldwide Energy Resources. (2025, October 22). https://power.larc.nasa.gov/

OMM. (1951). *OMM Annual Report for 1951*. World Meteorological Organization. https://library.wmo.int/records/item/55407-annual-report-for-1951?offset=56

Pebesma, E. (2018). *Simple features for R: Standardized support for spatial vector data*. The R Journal,*10*(1),439–446. https://doi.org/10.32614/RJ-2018-009

Pebesma, E., & Bivand, R. (2023). *Spatial data science: With applications in R*. Chapman and Hall/CRC. https://doi.org/10.1201/9780429459016

Peterson, T. C., Easterling, D. R., Karl, T. R., Groisman, P., Nicholls, N., Plummer, N., Torok, S., Auer, I., Boehm, R., Gullett, D., Vincent, L., Heino, R., Tuomenvirta, H., Mestre, O., Szentimrey, T., Salinger, J., Førland, E. J., Hanssen-Bauer, I., Alexandersson, H., … Parker, D. (1998). *Homogeneity adjustments ofin situ atmospheric climate data: A review*. International Journal of Climatology, 18(13), 1493–1517. https://doi.org/10.1002/(SICI)1097-0088(19981115)18:13%253C1493::AID-JOC329%253E3.0.CO;2-T

Quansah, A. D., Boakye, P., Quansah, D. A., Mensah, L. D., Junior, P. A., Quansah, E., & Mensah, P. (2024). *Site adaptation of NASA-POWER reanalysis solar radiation products for tropical climates in Ghana using bias correction for clean energy application*. Research Square. https://doi.org/10.21203/rs.3.rs-4571887/v1

Quarto Development Team. (2024). *Quarto: Open-source scientific and technical publishing system* [Manual]. Posit Software, PBC. https://quarto.org/

Rabah MAYOUF & Mohamed Tahar HANAFI. (2025). *Assessing drought dynamics in Northeastern Algeria using the vegetation health index derived from Modis Data.* Carpathian Journal of Earth and Environmental Sciences, 20(1), 19–26. https://doi.org/10.26471/cjees/2025/020/310

Rienecker, M. M., Suarez, M. J., Gelaro, R., Todling, R., Bacmeister, J., Liu, E., Bosilovich, M. G., Schubert, S. D., Takacs, L., Kim, G.-K., Bloom, S., Chen, J., Collins, D., Conaty, A., Silva, A. da, Gu, W., Joiner, J., Koster, R. D., Lucchesi, R., … Woollen, J. (2011). *MERRA: NASA's Modern-Era Retrospective Analysis for Research and*

*Applications. Journal of Climate, 24(1*4), 3624–3648. https://doi.org/10.1175/JCLI-D-11-00015.1

Rodrigues, G. C., & Braga, R. P. (2021a). E*stimation of Daily Reference Evapotranspiration from NASA POWER Reanalysis Products in a Hot Summer Mediterranean Climate*. Agronomy, 11(10),10. https://doi.org/10.3390/agronomy11102077

Rodrigues, G. C., & Braga, R. P. (2021b). *Evaluation of NASA POWER Reanalysis Products to Estimate Daily Weather Variables in a Hot Summer Mediterranean Climate*. Agronomy, 11(6), 6. https://doi.org/10.3390/agronomy11061207

RStudio Team. (2024). *RStudio: Integrated development environment for R* [Manual]. RStudio, PBC. https://www.rstudio.com/

Sarfaraz, A. (2017). *Impact of climate-tectonic interaction on terrain characteristics of the watersheds in Western Himalaya*. Carpathian Journal of Earth and Environmental Sciences, 1*2*(1).

Serbaji, M. M., Bouaziz, M., & Weslati, O. (2023). *Soil Water Erosion Modeling in Tunisia Using RUSLE and GIS Integrated Approaches and Geospatial Data.* Land, 12(3), Article 3. https://doi.org/10.3390/land12030548

Sparks, A. H. (2018). *nasapower*: *A NASA POWER global meteorology, surface solar energy and climatology data client for R.* The Journal of Open Source Software, 3(30), 1035. https://doi.org/10.21105/joss.01035

Tan, M. L., Armanuos, A. M., Ahmadianfar, I., Demir, V., Heddam, S., Al-Areeq, A. M., Abba, S. I., Halder, B., Cagan Kilinc, H., & Yaseen, Z. M. (2023). *Evaluation of NASA POWER and ERA5-Land for estimating tropical precipitation and temperature extremes.* Journal of Hydrology, 624, 129940. https://doi.org/10.1016/j.jhydrol.2023.129940

Teutschbein, C., & Seibert, J. (2012). *Bias correction of regional climate model simulations for hydrological climate-change impact studies: Review and evaluation of different methods. J*ournal of Hydrology, 456–457, 12–29. https://doi.org/10.1016/j.jhydrol.2012.05.052

Wei, G., Lü, H., T. Crow, W., Zhu, Y., Wang, J., & Su, J. (2018). *Evaluation of Satellite-Based Precipitation Products from IMERG V04A and V03D, CMORPH and TMPA with Gauged Rainfall in Three Climatologic Zones in China*. *R*emote Sensing, 10(1), 30. https://doi.org/10.3390/rs10010030

Wickham, H., Averick, M., Bryan, J., Chang, W., McGowan, L. D., François, R., Grolemund, G., Hayes, A., Henry, L., Hester, J., Kuhn, M., Pedersen, T. L., Miller, E., Bache, S. M., Müller, K., Ooms, J., Robinson, D., Seidel, D. P., Spinu, V., … Yutani, H. (2019). *Welcome to the Tidyverse*. Journal of Open Source Software, 4(43), 1686. https://doi.org/10.21105/joss.01686

Wilkinson, M. D., Dumontier, M., Aalbersberg, Ij. J., Appleton, G., Axton, M., Baak, A., Blomberg, N., Boiten, J.-W., da Silva Santos, L. B., Bourne, P. E., Bouwman, J., Brookes, A. J., Clark, T., Crosas, M., Dillo, I., Dumon, O., Edmunds, S., Evelo, C. T., Finkers, R., … Mons, B. (2016). *The FAIR Guiding Principles for scientific data management and stewardship.* Scientific Data, 3(1), 160018. https://doi.org/10.1038/sdata.2016.18

Wilks, D. S. (2019). *Statistical methods in the atmospheric sciences* (Fourth Edition). Elsevier. https://doi.org/10.1016/B978-0-12-815823-4.00001-8

World Meteorological Organization (WMO). (2022). *WMO Unified Data Policy* (General Information, p. 32). WMO. https://library.wmo.int/idurl/4/58009

Zhang, L., Zhang, G., & Sun, G. (2017). *Variation trend of dry-wet climatic factors and correlation with wetlands in Western Jilin Province, Chinses.* Carpathian Journal of Earth and Environmental Sciences, 12(1), 131–139.

Zhang, T., Chandler, W. S., Hoell, J. M., Westberg, D., Whitlock, C. H., & Stackhouse, P. W. (2009). *A Global Perspective on Renewable Energy Resources: Nasa's Prediction of Worldwide Energy Resources (Power) Project*. In D. Y. Goswami & Y. Zhao (Eds.), *Proceedings of ISES World Congress 2007 (Vol. I – Vol. V)* (pp. 2636–2640). Springer. https://doi.org/10.1007/978-3-540-75997-3_532

Received: 03.01. 2026
Revised: 11.02. 2026
Accepted: 16.02.2026
Published: 18. 02. 2026